

Energy Dependence of Directed Flow in Au+Au Collisions from a Multi-phase Transport Model

J. Y. Chen*

*Institution of Particle Physics, Huazhong Normal University(CCNU), Wuhan 430079, P.R.China and
The Key Laboratory of Quark and Lepton Physics (Huazhong Normal University),
Ministry of Education, Wuhan, Hubei, 430079, P.R.China*

J. X. Zuo†

Institute of High Energy Physics, CAS, Beijing 100049, P.R.China

X. Z. Cai

Shanghai Institute of Applied Physics, Shanghai, 201800, P.R.China

F. Liu

*Institution of Particle Physics, Huazhong Normal University(CCNU), Wuhan 430079, P.R.China and
The Key Laboratory of Quark and Lepton Physics (Huazhong Normal University),
Ministry of Education, Wuhan, Hubei, 430079, P.R.China*

Y. G. Ma

Shanghai Institute of Applied Physics, Shanghai, 201800, P.R.China

A. H. Tang

Physics Department, Brookhaven National Lab., Upton, NY 11973, USA

(Dated: February 14, 2019)

Directed flow of charged hadron and identified particles have been studied in the framework of a multi-phase transport (AMPT) model, for $^{197}\text{Au}+^{197}\text{Au}$ collisions at $\sqrt{s_{NN}}=200, 130, 62.4, 39, 17.2$ and 9.2 GeV. The rapidity, centrality and energy dependence of directed flow for charged particles over a wide rapidity range are presented. AMPT model gives the right $v_1(y)$ slope, as well as its trend as a function of energy, while underestimate the magnitude. Within AMPT model, proton v_1 slope is found to change its sign when the energy increases to 130 GeV - a feature that is consistent with “anti-flow”. The hadronic re-scattering is found having little effect on v_1 at top RHIC energies. These studies can help us to understand the collective dynamics at early time in relativistic heavy ion collisions, and they can also be served as references for the RHIC Beam Energy Scan program.

PACS numbers: 25.75.Ld, 25.75.Nq, 25.75.Dw

I. INTRODUCTION

The anisotropic flow is one of the key observable in characterizing properties of the dense and hot medium created in relativistic heavy-ion collisions[1], and it is quantified by Fourier coefficients when expanding particle’s azimuthal distribution with respect to the reaction plane[2]:

$$E \frac{d^3 N}{d^3 p} = \frac{1}{2\pi} \frac{d^2 N}{p_T dp_T dy} \left(1 + \sum_{n=1}^{\infty} 2v_n \cos n\phi \right) \quad (1)$$

where ϕ denotes the angle between the particle’s azimuthal angle in momentum space and the reaction plane angle. The sine terms in Fourier expansions vanish due to the reflection symmetry with respect to the reaction

plane. The various coefficients in this expansion can be defined as:

$$v_n = \langle \cos n\phi \rangle \quad (2)$$

The first and the second coefficient are named as directed flow (v_1) and elliptic flow(v_2), respectively, and they play important roles in describing the collective expansion in azimuthal space. Elliptic flow is produced by the conversion of the initial coordinate-space anisotropy into the momentum-space anisotropy, due to the developed large in-plane pressure gradient. Elliptic flow depends strongly on the re-scattering of the system constituents, thus it is sensitive to the degree of thermalization[3] of the system at early time. Directed flow, which is the focus of this study, describes the “side splash” of particles away from mid-rapidity[4], and it probes the dynamics of the system in the longitudinal direction. Since directed flow is generated very early, it brings the information from the foremost early collective motion of the system. The shapes of directed flow, in

*Electronic address: chenjy@iopp.cnu.edu.cn

†Electronic address: zuojx@ihep.ac.cn

particular those for identified particles, are of special interest because they are sensitive to the equation of state (EOS) and may carry phase transition signal[5].

The study of energy dependence of directed flow has implications in many aspects. First, because that directed flow has a unique, pre-equilibrium origin, it is expected to behave differently than other soft observable which show a “entropy-driven” multiplicity scaling[6]. It has been shown by STAR[7] that at top RHIC energies, directed flow is independent of system size, while it has an energy dependence. For a comprehensive study of the subject, it is necessary to extend the study of the energy dependence of directed flow in a wider range of energy. Secondly, experiments at RHIC (PHENIX and STAR) have planned to look for the existence of QCD phase boundary and the possible critical point by colliding heavy ions at various incident beam energies[8, 9, 10]. A non-monotonic dependence of variables on $\sqrt{s_{NN}}$ and an increase in event-by-event fluctuations should become apparent near the critical point[8]. Directed flow is generated during the nuclear passage time ($2R/\gamma \sim 0.1 fm/c$) and it probes the onset of bulk collective dynamics in the earlier stage of the collision. As a suggested signature of first order phase transition[5], directed flow is sensitive to the creation of the critical point and it plays an important role in the proposed beam energy scan program.

In this paper, directed flow from AMPT model for 6 energies are presented, they are, 9.2, 17.3, 39, 62.4, 130 and 200 GeV. The comparison to measurements from STAR and PHOBOS are made at top energies. Particle type dependence over a wide rapidity range is discussed. This study will deepen our understanding the energy dependence of directed flow, and it can be also served as a valuable reference for the RHIC Beam Energy Scan program.

II. THE AMPT MODEL

The AMPT model consists of four main components[11]: initial conditions, partonic interactions, conversion from partonic matter to hadronic matter, and hadronic interactions. The initial conditions, which include the spatial and momentum distributions of the mini-jet partons and soft string excitations, are obtained from the HIJING model[13]. Scatterings among partons are modeled by Zhang’s parton cascade(ZPC)[14], which includes two-body scatterings with cross sections from pQCD with screening masses. In the default AMPT model[15], partons are recombined with their parent strings when they stop interacting, and the resulting strings fragment into hadrons according to the Lund string fragmentation model[16]. In the AMPT model with string melting[17], a quark coalescence is used instead to combine partons into hadrons. The dynamics of the subsequent hadronic matter is described by the ART (a relativistic transport) model[18] with modifications and extensions.

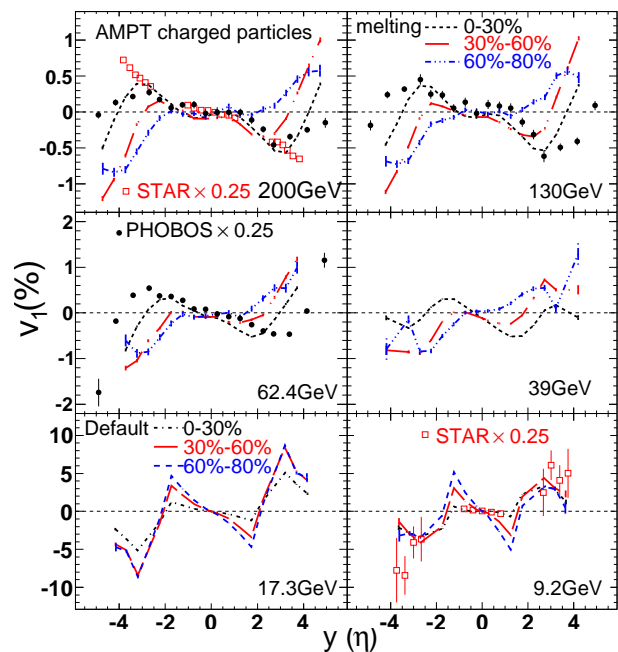


FIG. 1: Rapidity dependence of the v_1 for charged particles in the AMPT model compared with STAR and PHOBOS data (plotted as a function of η) in the Au+Au collisions at $\sqrt{s_{NN}} = 200$ GeV. The dashed lines showed AMPT result from different centrality: 0-30%(black), 30%-60%(red), 60%-80%(blue).

For results presented in this paper, directed flow of charged particles at RHIC energies larger than 39 GeV (including 39 GeV) are based on the AMPT model with string melting scenario[11], while results from lower energies are based on the AMPT default scenario[15]. The AMPT model with string melting scenario is believed to be much more appropriate than the one with default scenario in describing collisions at top energies at RHIC[19, 20], because the energy density in these collisions is much higher than the critical density for the QCD phase transition. The evolution dynamics of the hadron matter will be described by a modified ART model. Following [21], the parton cross section is chosen as 3mb. All the errors presented here are statistical errors.

III. ANALYSIS AND RESULTS

In Fig. 1, directed flow of charged particles from AMPT are shown as a function of rapidity, for collision energies of 200, 130, 62.4, 39, 17.2 and 9.2 GeV. The centrality is divided into three bins, namely, 0-30%, 30%-60% and 60%-80%, based on the impact parameter (b) distribution. The calculations with string melting scenario is used for high energies (200, 130, 62.4, 39 GeV) while for low energies (17.2 and 9.2 GeV) calculations are performed with default scenario. The reason for such

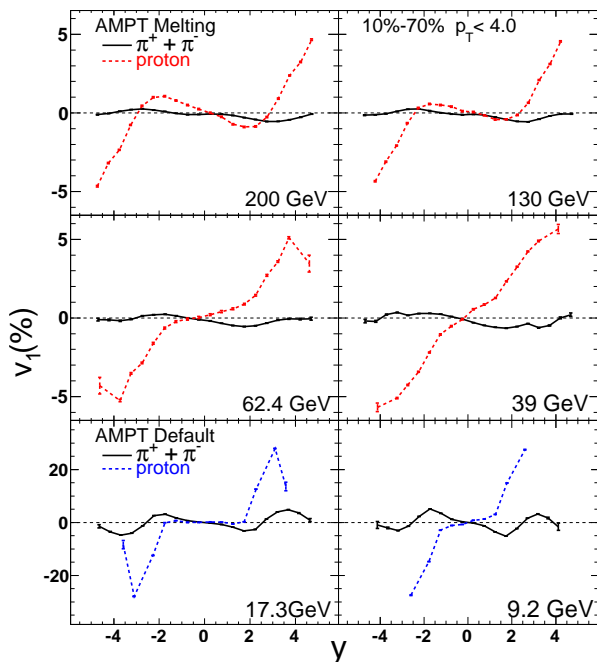


FIG. 2: Proton (solid lines) and Pion (dashed lines) $v_1(y)$ from AMPT at centrality 10%-70%.

choice is because that, it is argued [21] that the string melting should be used to explain flow around midrapidity at top RHIC energies, and default setting describes data at 9.2 GeV the best. More discussion on different AMPT configurations can be found later in this paper. All results are obtained by integrating over transverse momentum (p_T) up to 4.0 GeV/c. Experimental results from STAR[7, 22] and PHOBOS[23] are also shown for comparison. The charged hadron v_1 measured by PHOBOS experiment is for 0-40% central collisions, and the results measured by STAR experiment are for centrality 30%-60% at 200GeV, and centrality 0-60% at 9.2GeV. In general, AMPT gives larger v_1 at low energies than that at high energies, the same trend has been seen in data. At top RHIC energies, AMPT underestimated v_1 , due to the turn-off of mean-field potentials in ART when implemented in AMPT to describe the hadronic scattering[11]. However, in the rapidity range of $[-2.0, 2.0]$, the shape of v_1 between AMPT calculations and experimental data are in good agreement – this can be seen by scaling experimental result with a factor of 0.25.

The particle type dependence of directed flow is shown in Fig. 2. The different sign of v_1 between pion and proton at low energies can be understood as nucleon shadowing and baryon stopping[24, 25]. In general the magnitude of v_1 slope at midrapidity decreases with the increasing of energy. This effect is most profound for protons, for which the slope keep decreasing and when the energy is high enough, it changes its sign and protons begin to flow together with pions. This is consistent with the “anti-flow” scenario[26], in which the “bounce-off” mo-

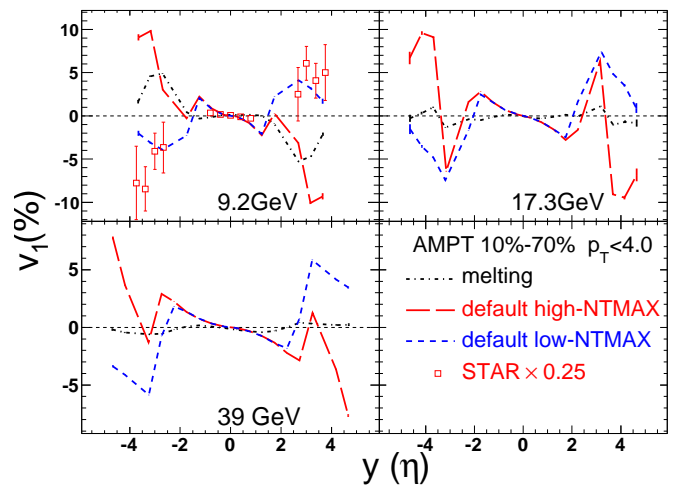


FIG. 3: Charged particles $v_1(y)$ from centrality 10%-70% for 9.2GeV (upper left panel), 17.3GeV (upper right panel) and 39GeV (down left panel). The dashed lines show three AMPT version: string melting scenario (black), default scenario with high-NTMAX (red) and low-NTMAX (blue). Experimental data points from STAR are plotted as a function of η .

tion and transverse expansion of nucleons compete with each other around midrapidity, and when the transverse expansion is strong enough (e.g., at top RHIC energies), it overcomes the “bounce-off” motion and causes protons to change its sign of directed flow.

To illustrate the effect on v_1 due to different configurations in AMPT, in Fig. 3 we present the directed flow of charged hadrons in low energy collisions, from AMPT calculations with the string melting scenario and the default scenario. The similar study for higher energies can be found in [21]. The calculation with string melting yield the smallest v_1 slope around midrapidity and is close to data. Two different default scenario are also studied: one is calculated with NTMAX=2500 (high-NTMAX), and the other, NTMAX=150 (low-NTMAX). NTMAX stands for the number of time-steps for hadron cascade, see detail in paper [11]. A large NTMAX means a thoroughly developed hadron cascade, as $0.2\text{fm}/c * \text{NTMAX}$ is the termination time, in the center of mass frame, of hadron cascade in AMPT model. The comparison, for low energies, of v_1 calculated between low-NTMAX and high-NTMAX indicates that v_1 can change its sign at large rapidity if the time for hadronic cascade is long enough. In default AMPT, NTMAX has to be much larger than 150 in order to describe v_1 at large rapidity. The disagreement between data and the calculation made with high-NTMAX is mostly due to the lack of mean-field in the hadron cascade in AMPT, which is a considerable effect at low energies when the nuclei passage time is not negligible (compared to that at high energies). The AMPT calculation with high-NTMAX at high energy has been presented in [12], in this paper, we address the comparison around midrapidity only, and re-

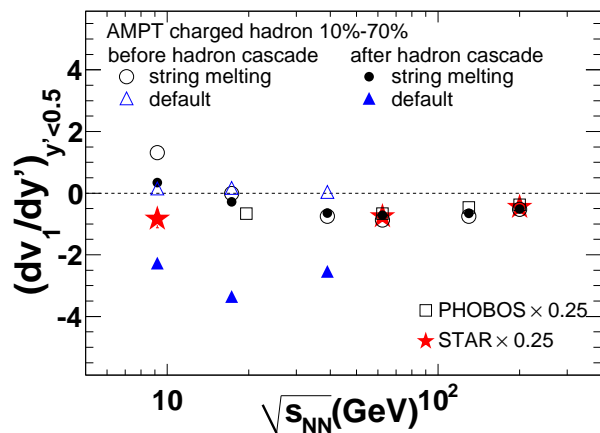


FIG. 4: Charged hadrons' slope dv_1/dy' in the mid-rapidity $|y'| < 0.5$ as a function of incident-energy. The data are taken from STAR(stars) and PHOBOS(squares) and scaled by a factor 0.25. The AMPT calculations with string melting before ART are depicted with open circles and after hadron cascade are depicted with full circles. The open triangles depict the default AMPT calculations before ART and the full triangles depict after hadron cascade.

sults presented in this paper are made with low-NTMAX unless otherwise specified.

The energy dependence of charged particle directed flow, calculated with AMPT model, is shown in Fig. 4. Experimental data are also shown for comparison. The centrality for which the calculation is performed is 10%-70%. The centrality for PHOBOS data from different energies is 0-40% while the centrality selection for STAR data are 0-60% for 9.2 GeV, 10%-70% for 62.4 GeV, and 30%-60% for 200 GeV. To obtain the integrated v_1 , one needs to fold in the spectra at different energies, which brings in additional layer of systematics. Thus instead, we present the slope of $v_1(y)$ around mid-rapidity ($|y'| < 0.5$) extracted from the normalized ($y' = y/y_{beam}$) rapidity distribution, where y_{beam} is the beam rapidity. For the energy range that string melting is used (39 GeV and above), all the AMPT calculations underestimate the experimental data, however, they predict the right trend of the energy dependence. For the low energies at 9.2 GeV, calculations with string melting did a poor job, the

calculation with default AMPT improves the result in the right direction yet still not be able to explain the data. The hadron re-scattering effect on directed flow v_1 can be seen by switching off hadron cascade in AMPT calculation. Comparing the difference between result with hadron cascade (open symbols) and without (solid symbols), it is found that hadronic cascade has a significant effect for low energy results but little for that of high energies. This can be understood as that, when the energy is high enough, the hadron re-scattering become less important due to the presence of strong collective motion built up beforehand.

IV. SUMMARY AND CONCLUSIONS

In this paper v_1 calculated from AMPT model for different energies are discussed. It is found that AMPT model gives the right shape of v_1 versus y while underestimates the magnitude, possibly due to the lack of mean-field in its hadron cascade. In AMPT, the proton v_1 slope changes its sign when the energy increases to 130 GeV and begin to have the same sign as that of pions, as expected in the ‘‘anti-flow’’ scenario. The effect on v_1 due to string melting, low-NTMAX and high-NTMAX are illustrated. The energy dependence of v_1 slope at midrapidity is compared to experimental data, and AMPT can describe the trend of energy dependence while missed the magnitude by a fraction of 75%. The hadronic rescattering effect is found to be less important at high energies as the strong collective motion becomes to be the dominant dynamics.

Acknowledgments

Authors greatly thank Zi-Wei Lin for useful discussions and kindly providing comments to this paper. This work was supported in part the National Natural Science Foundation of China under Grant No. 10775058 & No. 10610285, MOE of China under Grant No. IRT0624 and MOST of China under Grant No. 2008CB817707, and the Knowledge Innovation Project of the Chinese Academy of Sciences under Grant Nos. KJCX2-YW-A14 and and KJCX3-SYW-N2.

[1] For a recent review, see : S. A. Voloshin, A. M. Poskanzer and R. Snellings, arXiv: 0909.2949 [nucl-ex].
 [2] A. M. Poskanzer and S. A. Voloshin, Phys. Rev. C **58** 1671 (1998).
 [3] P. Kolb, J. Sollfrank, and U. Heinz, Phys. Rev. C **62** 054909 (2000).
 [4] H. Sorge, Phys. Rev. Lett. **78** 2309 (1997).
 [5] H. Stoecker, Nucl. Phys. A **750** 121-147 (2005).
 [6] A. H. Tang, J. Phys. G **34**, S277 (2007); H. Song and

U. Heinz, Phys. Rev. C **78** 024902 (2008); J. Chen (for the STAR Collaboration) J. Phys. G **35** 044072 (2008).
 [7] B. I. Abelev *et al.* (STAR experiment), Phys. Rev. Lett. **101** 252301 (2008).
 [8] P. Sorensen (for STAR Collaboration) arXiv: 0701028v1 [nucl-ex].
 [9] G. Odyniec (for STAR Collaboration), J. Phys. G **35** 104164 (2008).
 [10] T. Sakaguchi (for PHENIX Collaboration),

- PHENIX plans for RHIC low energy run, talk for *the 5th International Workshop on Critical Point and Onset of Deconfinement (CPOD)*, [http://quark.phy.bnl.gov/~karsch/agenda_cpod.html].
- [11] Z. W. Lin, C. M. Ko, B. A. Li, B. Zhang, and S. Pal, Phys. Rev. C **72** 064901 (2005).
 - [12] L. W. Chen, V. Greco, C. M. Ko and P. Kolb, Phys. Lett. B **605** 95 (2005).
 - [13] X. N. Wang and M. Gyulassy, Phys. Rev. D **45** 844 (1992); M. Gyulassy and X. N. Wang, Comput. Phys. Commun. **83** 307 (1994).
 - [14] B. Zhang, Comput. Phys. Commun. **109** 193 (1998).
 - [15] Z. W. Lin and C. M. Ko, Phys. Rev. C **68** 054904 (2003).
 - [16] B. Andersson, G. Gustafson and B. Soderbery, Z. Phys. C **20** 317 (1983).
 - [17] Z. W. Lin and C. M. Ko, J. Phys. G **30** S263 (2004).
 - [18] B. Li, A. T. Sustich, B. Zhang and C. M. Ko, Int. J. Mod. Phys. E **10** 267 (2001).
 - [19] J. H. Chen et.al Phys. Rev. C **74** 064902 (2006).
 - [20] J. X. Zuo et.al Eur. Phys. J. C **55** 463 (2008).
 - [21] C. M. Ko and L. W. Chen Nucl. Phys. A **774** 527 (2006).
 - [22] B. I. Abelev *et al.* (STAR Collaboration), arXiv: 0909.4131 [nucl-ex]; L. Kumar (for the STAR Collaboration) J. Phys. G **36** 064066 (2009); J. Y. Chen (for STAR Collaboration), arXiv: 0910.0556 [nucl-ex].
 - [23] B. B. Back *et al.* (PHOBOS Collaboration), Phys. Rev. Lett. **97** 012301 (2006).
 - [24] R. J. M. Snellings, H. Sorge, S. A. Voloshin, F. Q. Wang, and N. Xu, Phys. Rev. Lett. **84** 2803 (2000).
 - [25] H. Liu, S. Panitkin and N. Xu, Phys. Rev. C **59** 348 (1998).
 - [26] J. Brachmann *et al.*, Phys. Rev. C **61** 024909 (2000); L.P. Csernai and D.Rohrich, Phys. Lett. B **458** 454 (1999).

Energy Dependence of Directed Flow in Au+Au Collisions from a Multi-phase Transport Model

J. Y. Chen*

*Institution of Particle Physics, Huazhong Normal University(CCNU), Wuhan 430079, P.R.China and
The Key Laboratory of Quark and Lepton Physics (Huazhong Normal University),
Ministry of Education, Wuhan, Hubei, 430079, P.R.China*

J. X. Zuo†

Institute of High Energy Physics, CAS, Beijing 100049, P.R.China

X. Z. Cai

Shanghai Institute of Applied Physics, Shanghai, 201800, P.R.China

F. Liu

*Institution of Particle Physics, Huazhong Normal University(CCNU), Wuhan 430079, P.R.China and
The Key Laboratory of Quark and Lepton Physics (Huazhong Normal University),
Ministry of Education, Wuhan, Hubei, 430079, P.R.China*

Y. G. Ma

Shanghai Institute of Applied Physics, Shanghai, 201800, P.R.China

A. H. Tang

Physics Department, Brookhaven National Lab., Upton, NY 11973, USA

(Dated: February 14, 2019)

Directed flow of charged hadron and identified particles have been studied in the framework of a multi-phase transport (AMPT) model, for $^{197}\text{Au}+^{197}\text{Au}$ collisions at $\sqrt{s_{NN}}=200, 130, 62.4, 39, 17.2$ and 9.2 GeV. The rapidity, centrality and energy dependence of directed flow for charged particles over a wide rapidity range are presented. AMPT model gives the right $v_1(y)$ slope, as well as its trend as a function of energy, while underestimate the magnitude. Within AMPT model, proton v_1 slope is found to change its sign when the energy increases to 130 GeV - a feature that is consistent with “anti-flow”. The hadronic re-scattering is found having little effect on v_1 at top RHIC energies. These studies can help us to understand the collective dynamics at early time in relativistic heavy ion collisions, and they can also be served as references for the RHIC Beam Energy Scan program.

PACS numbers: 25.75.Ld, 25.75.Nq, 25.75.Dw

I. INTRODUCTION

The anisotropic flow is one of the key observable in characterizing properties of the dense and hot medium created in relativistic heavy-ion collisions[1], and it is quantified by Fourier coefficients when expanding particle’s azimuthal distribution with respect to the reaction plane[2]:

$$E \frac{d^3 N}{d^3 p} = \frac{1}{2\pi} \frac{d^2 N}{p_T dp_T dy} \left(1 + \sum_{n=1}^{\infty} 2v_n \cos n\phi \right) \quad (1)$$

where ϕ denotes the angle between the particle’s azimuthal angle in momentum space and the reaction plane angle. The sine terms in Fourier expansions vanish due to the reflection symmetry with respect to the reaction

plane. The various coefficients in this expansion can be defined as:

$$v_n = \langle \cos n\phi \rangle \quad (2)$$

The first and the second coefficient are named as directed flow (v_1) and elliptic flow(v_2), respectively, and they play important roles in describing the collective expansion in azimuthal space. Elliptic flow is produced by the conversion of the initial coordinate-space anisotropy into the momentum-space anisotropy, due to the developed large in-plane pressure gradient. Elliptic flow depends strongly on the re-scattering of the system constituents, thus it is sensitive to the degree of thermalization[3] of the system at early time. Directed flow, which is the focus of this study, describes the “side splash” of particles away from mid-rapidity[4], and it probes the dynamics of the system in the longitudinal direction. Since directed flow is generated very early, it brings the information from the foremost early collective motion of the system. The shapes of directed flow, in

*Electronic address: chenjy@iopp.cnu.edu.cn

†Electronic address: zuojx@ihep.ac.cn

particular those for identified particles, are of special interest because they are sensitive to the equation of state (EOS) and may carry phase transition signal[5].

The study of energy dependence of directed flow has implications in many aspects. First, because that directed flow has a unique, pre-equilibrium origin, it is expected to behave differently than other soft observable which show a “entropy-driven” multiplicity scaling[6]. It has been shown by STAR[7] that at top RHIC energies, directed flow is independent of system size, while it has an energy dependence. For a comprehensive study of the subject, it is necessary to extend the study of the energy dependence of directed flow in a wider range of energy. Secondly, experiments at RHIC (PHENIX and STAR) have planned to look for the existence of QCD phase boundary and the possible critical point by colliding heavy ions at various incident beam energies[8, 9, 10]. A non-monotonic dependence of variables on $\sqrt{s_{NN}}$ and an increase in event-by-event fluctuations should become apparent near the critical point[8]. Directed flow is generated during the nuclear passage time ($2R/\gamma \sim 0.1 fm/c$) and it probes the onset of bulk collective dynamics in the earlier stage of the collision. As a suggested signature of first order phase transition[5], directed flow is sensitive to the creation of the critical point and it plays an important role in the proposed beam energy scan program.

In this paper, directed flow from AMPT model for 6 energies are presented, they are, 9.2, 17.3, 39, 62.4, 130 and 200 GeV. The comparison to measurements from STAR and PHOBOS are made at top energies. Particle type dependence over a wide rapidity range is discussed. This study will deepen our understanding the energy dependence of directed flow, and it can be also served as a valuable reference for the RHIC Beam Energy Scan program.

II. THE AMPT MODEL

The AMPT model consists of four main components[11]: initial conditions, partonic interactions, conversion from partonic matter to hadronic matter, and hadronic interactions. The initial conditions, which include the spatial and momentum distributions of the mini-jet partons and soft string excitations, are obtained from the HIJING model[13]. Scatterings among partons are modeled by Zhang’s parton cascade(ZPC)[14], which includes two-body scatterings with cross sections from pQCD with screening masses. In the default AMPT model[15], partons are recombined with their parent strings when they stop interacting, and the resulting strings fragment into hadrons according to the Lund string fragmentation model[16]. In the AMPT model with string melting[17], a quark coalescence is used instead to combine partons into hadrons. The dynamics of the subsequent hadronic matter is described by the ART (a relativistic transport) model[18] with modifications and extensions.

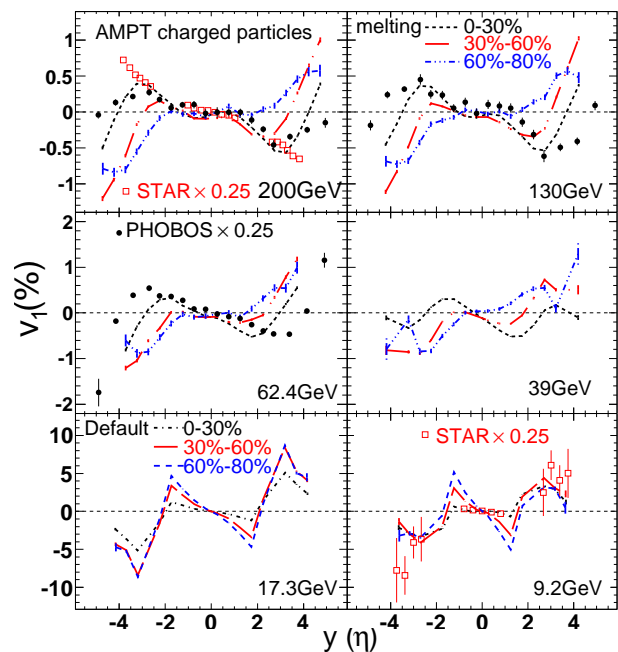


FIG. 1: Rapidity dependence of the v_1 for charged particles in the AMPT model compared with STAR and PHOBOS data (plotted as a function of η) in the Au+Au collisions at $\sqrt{s_{NN}} = 200$ GeV. The dashed lines showed AMPT result from different centrality: 0-30%(black), 30%-60%(red), 60%-80%(blue).

For results presented in this paper, directed flow of charged particles at RHIC energies larger than 39 GeV (including 39 GeV) are based on the AMPT model with string melting scenario[11], while results from lower energies are based on the AMPT default scenario[15]. The AMPT model with string melting scenario is believed to be much more appropriate than the one with default scenario in describing collisions at top energies at RHIC[19, 20], because the energy density in these collisions is much higher than the critical density for the QCD phase transition. The evolution dynamics of the hadron matter will be described by a modified ART model. Following [21], the parton cross section is chosen as 3mb. All the errors presented here are statistical errors.

III. ANALYSIS AND RESULTS

In Fig. 1, directed flow of charged particles from AMPT are shown as a function of rapidity, for collision energies of 200, 130, 62.4, 39, 17.2 and 9.2 GeV. The centrality is divided into three bins, namely, 0-30%, 30%-60% and 60%-80%, based on the impact parameter (b) distribution. The calculations with string melting scenario is used for high energies (200, 130, 62.4, 39 GeV) while for low energies (17.2 and 9.2 GeV) calculations are performed with default scenario. The reason for such

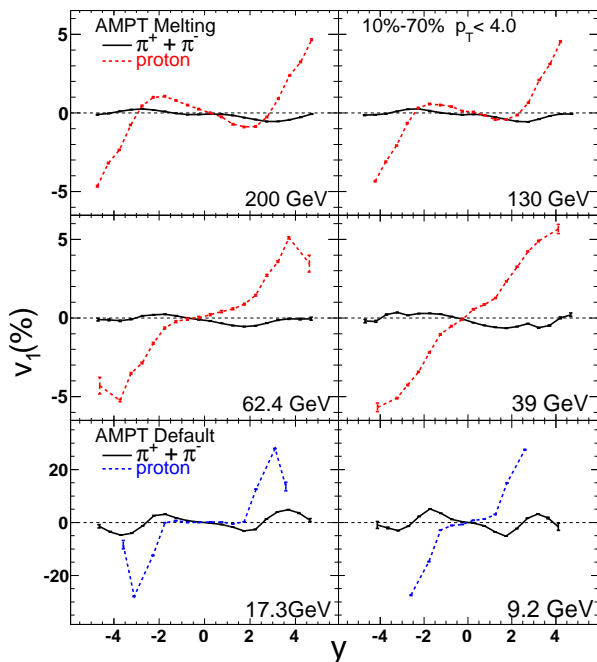


FIG. 2: Proton(solid lines) and Pion(dashed lines) $v_1(y)$ from AMPT at centrality 10%-70%.

choice is because that, it is argued [21] that the string melting should be used to explain flow around midrapidity at top RHIC energies, and default setting describes data at 9.2 GeV the best. More discussion on different AMPT configurations can be found later in this paper. All results are obtained by integrating over transverse momentum (p_T) up to 4.0 GeV/c. Experimental results from STAR[7, 22] and PHOBOS[23] are also shown for comparison. The charged hadron v_1 measured by PHOBOS experiment is for 0-40% central collisions, and the results measured by STAR experiment are for centrality 30%-60% at 200GeV, and centrality 0-60% at 9.2GeV. In general, AMPT gives larger v_1 at low energies than that at high energies, the same trend has been seen in data. At top RHIC energies, AMPT underestimated v_1 , due to the turn-off of mean-field potentials in ART when implemented in AMPT to describe the hadronic scattering[11]. However, in the rapidity range of $[-2.0, 2.0]$, the shape of v_1 between AMPT calculations and experimental data are in good agreement – this can be seen by scaling experimental result with a factor of 0.25.

The particle type dependence of directed flow is shown in Fig. 2. The different sign of v_1 between pion and proton at low energies can be understood as nucleon shadowing and baryon stopping[24, 25]. In general the magnitude of v_1 slope at midrapidity decreases with the increasing of energy. This effect is most profound for protons, for which the slope keep decreasing and when the energy is high enough, it changes its sign and protons begin to flow together with pions. This is consistent with the “anti-flow” scenario[26], in which the “bounce-off” mo-

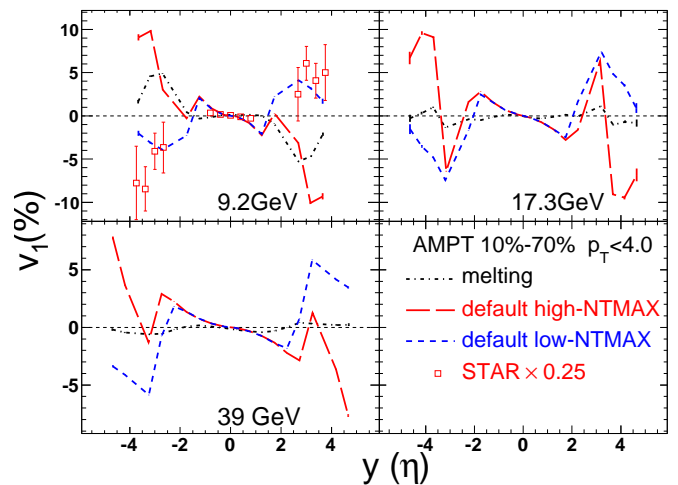


FIG. 3: Charged particles $v_1(y)$ from centrality 10%-70% for 9.2GeV(upper left panel),17.3GeV(upper right panel) and 39GeV(down left panel). The dashed lines show three AMPT version: string melting scenario(black), default scenario with high-NTMAX(red) and low-NTMAX(blue). Experimental data points from STAR are plotted as a function of η .

tion and transverse expansion of nucleons compete with each other around midrapidity, and when the transverse expansion is strong enough (e.g., at top RHIC energies), it overcomes the “bounce-off” motion and causes protons to change its sign of directed flow.

To illustrate the effect on v_1 due to different configurations in AMPT, in Fig. 3 we present the directed flow of charged hadrons in low energy collisions, from AMPT calculations with the string melting scenario and the default scenario. The similar study for higher energies can be found in [21]. The calculation with string melting yield the smallest v_1 slope around midrapidity and is close to data. Two different default scenario are also studied: one is calculated with NTMAX=2500 (high-NTMAX), and the other, NTMAX=150 (low-NTMAX). NTMAX stands for the number of time-steps for hadron cascade, see detail in paper [11]. A large NTMAX means a thoroughly developed hadron cascade, as $0.2\text{fm}/c \cdot \text{NTMAX}$ is the termination time, in the enter of mass frame, of hadron cascade in AMPT model. The comparison, for low energies, of v_1 calculated between low-NTMAX and high-NTMAX indicates that v_1 can change its sign at large rapidity if the time for hadronic cascade is long enough. In default AMPT, NTMAX has to be much larger than 150 in order to describe v_1 at large rapidity. The disagreement between data and the calculation made with high-NTMAX is mostly due to the lack of mean-field in the hadron cascade in AMPT, which is a considerable effect at low energies when the nuclei passage time is not negligible (compared to that at high energies). The AMPT calculation with high-NTMAX at high energy has been presented in [12], in this paper, we address the comparison around midrapidity only, and re-

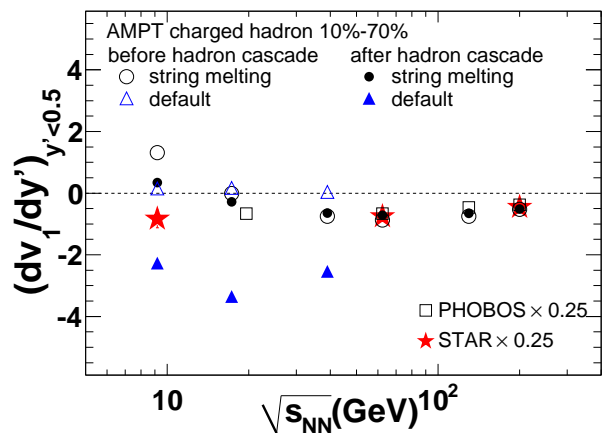


FIG. 4: Charged hadrons' slope dv_1/dy' in the mid-rapidity $|y'| < 0.5$ as a function of incident-energy. The data are taken from STAR(stars) and PHOBOS(squares) and scaled by a factor 0.25. The AMPT calculations with string melting before ART are depicted with open circles and after hadron cascade are depicted with full circles. The open triangles depict the default AMPT calculations before ART and the full triangles depict after hadron cascade.

sults presented in this paper are made with low-NTMAX unless otherwise specified.

The energy dependence of charged particle directed flow, calculated with AMPT model, is shown in Fig. 4. Experimental data are also shown for comparison. The centrality for which the calculation is performed is 10%-70%. The centrality for PHOBOS data from different energies is 0-40% while the centrality selection for STAR data are 0-60% for 9.2 GeV, 10%-70% for 62.4 GeV, and 30%-60% for 200 GeV. To obtain the integrated v_1 , one needs to fold in the spectra at different energies, which brings in additional layer of systematics. Thus instead, we present the slope of $v_1(y)$ around mid-rapidity ($|y'| < 0.5$) extracted from the normalized ($y' = y/y_{beam}$) rapidity distribution, where y_{beam} is the beam rapidity. For the energy range that string melting is used (39 GeV and above), all the AMPT calculations underestimate the experimental data, however, they predict the right trend of the energy dependence. For the low energies at 9.2 GeV, calculations with string melting did a poor job, the

calculation with default AMPT improves the result in the right direction yet still not be able to explain the data. The hadron re-scattering effect on directed flow v_1 can be seen by switching off hadron cascade in AMPT calculation. Comparing the difference between result with hadron cascade (open symbols) and without (solid symbols), it is found that hadronic cascade has a significant effect for low energy results but little for that of high energies. This can be understood as that, when the energy is high enough, the hadron re-scattering become less important due to the presence of strong collective motion built up beforehand.

IV. SUMMARY AND CONCLUSIONS

In this paper v_1 calculated from AMPT model for different energies are discussed. It is found that AMPT model gives the right shape of v_1 versus y while underestimates the magnitude, possibly due to the lack of mean-field in its hadron cascade. In AMPT, the proton v_1 slope changes its sign when the energy increases to 130 GeV and begin to have the same sign as that of pions, as expected in the ‘‘anti-flow’’ scenario. The effect on v_1 due to string melting, low-NTMAX and high-NTMAX are illustrated. The energy dependence of v_1 slope at midrapidity is compared to experimental data, and AMPT can describe the trend of energy dependence while missed the magnitude by a fraction of 75%. The hadronic rescattering effect is found to be less important at high energies as the strong collective motion becomes to be the dominant dynamics.

Acknowledgments

Authors greatly thank Zi-Wei Lin for useful discussions and kindly providing comments to this paper. This work was supported in part the National Natural Science Foundation of China under Grant No. 10775058 & No. 10610285, MOE of China under Grant No. IRT0624 and MOST of China under Grant No. 2008CB817707, and the Knowledge Innovation Project of the Chinese Academy of Sciences under Grant Nos. KJCX2-YW-A14 and and KJCX3-SYW-N2.

[1] For a recent review, see : S. A. Voloshin, A. M. Poskanzer and R. Snellings, arXiv: 0909.2949 [nucl-ex].
 [2] A. M. Poskanzer and S. A. Voloshin, Phys. Rev. C **58** 1671 (1998).
 [3] P. Kolb, J. Sollfrank, and U. Heinz, Phys. Rev. C **62** 054909 (2000).
 [4] H.Sorge, Phys. Rev. Lett. **78** 2309 (1997).
 [5] H.Stocker, Nucl. Phys. A **750** 121-147 (2005).
 [6] A. H. Tang, J. Phys. G **34**, S277 (2007); H.Song and

U.Heinz, Phys. Rev. C **78** 024902 (2008); J. Chen (for the STAR Collaboration) J. Phys. G **35** 044072 (2008).
 [7] B. I. Abelev *et al.* (STAR experiment), Phys. Rev. Lett. **101** 252301 (2008).
 [8] P. Sorensen (for STAR Collaboration) arXiv: 0701028v1 [nucl-ex].
 [9] G. Odyniec (for STAR Collaboration), J. Phys. G **35** 104164 (2008).
 [10] T. Sakaguchi (for PHENIX Collaboration),

- PHENIX plans for RHIC low energy run, talk for *the 5th International Workshop on Critical Point and Onset of Deconfinement (CPOD)*, [http://quark.phy.bnl.gov/~karsch/agenda_cpod.html].
- [11] Z. W. Lin, C. M. Ko, B. A. Li, B. Zhang, and S. Pal, Phys. Rev. C **72** 064901 (2005).
- [12] L. W. Chen, V. Greco, C. M. Ko and P. Kolb, Phys. Lett. B **605** 95 (2005).
- [13] X. N. Wang and M. Gyulassy, Phys. Rev. D **45** 844 (1992); M. Gyulassy and X. N. Wang, Comput. Phys. Commun. **83** 307 (1994).
- [14] B. Zhang, Comput. Phys. Commun. **109** 193 (1998).
- [15] Z. W. Lin and C. M. Ko, Phys. Rev. C **68** 054904 (2003).
- [16] B. Andersson, G. Gustafson and B. Soderbery, Z. Phys. C **20** 317 (1983).
- [17] Z. W. Lin and C. M. Ko, J. Phys. G **30** S263 (2004).
- [18] B. Li, A. T. Sustich, B. Zhang and C. M. Ko, Int. J. Mod. Phys. E **10** 267 (2001).
- [19] J. H. Chen et.al Phys. Rev. C **74** 064902 (2006).
- [20] J. X. Zuo et.al Eur. Phys. J. C **55** 463 (2008).
- [21] C. M. Ko and L. W. Chen Nucl. Phys. A **774** 527 (2006).
- [22] B. I. Abelev *et al.* (STAR Collaboration), arXiv: 0909.4131 [nucl-ex]; Lokesh Kumar (for the STAR Collaboration) J. Phys. G **36** 064066 (2009); J. Y. Chen (for STAR Collaboration), arXiv: 0910.0556 [nucl-ex];
- [23] B. B. Back *et al.* (PHOBOS Collaboration), Phys. Rev. Lett. **97** 012301 (2006).
- [24] R. J. M. Snellings, H. Sorge, S. A. Voloshin, F. Q. Wang, and N. Xu, Phys. Rev. Lett. **84** 2803 (2000).
- [25] H. Liu, S. Panitkin and N. Xu, Phys. Rev. C **59** 348 (1998).
- [26] J. Brachmann *et al.*, Phys. Rev. C **61** 024909 (2000); L.P. Csernai and D.Rohrich, Phys. Lett. B **458** 454 (1999).

(Dated: February 14, 2019)

Abstract

